Turkish Journal of Computer and Mathematics Education Vol.12 No.12 (2021), 1913-1922

Research Article

Implementation of Fuzzy Controller for Capacitor Voltage Balance in MMC for PV based Induction Motor Drive

S. Prabhakara Chary [a], Dr. G. Venu Madhav [b] , Dr. T. Anil Kumar[c] , S.Saraswathi[d]

[a] PG Student Department of Electrical and Electronics Engineering, Anurag Group of Institutions (now Anurag University
[b,c,d] Professor Department of Electrical and Electronics Engineering, Anurag University, Venkatapur, Ghatkesar, Medchal–Malkajgiri District, Hyderabad, Telangana, India. 500 088.
Email: [a]prabhakarcharys@gmail.com ,[b]venumadhaveee@anurag.edu.in [c] thalluruanil@gmail.com
[d]saraswathieee@anurag.edu.in

Article History: Received: 11 January 2021; Revised: 12 February 2021; Accepted: 27 March 2021; Published online: 23 May 2021

Abstract: This paper discusses the capacitor voltage balance in MMC controlled by the space vector PWM technique. The proposed converter is included with four sub-modules each comprising a half-bridge converter with a DC link capacitor. An optimized control structure for capacitor voltage balance with the conventional PI controller is simulated compared to the updated visual system controller that changes the standard control. The converter function is analyzed with the comparison of settling times of the DC link capacitors voltages in each module. The performance of the induction motor is analyzed by connected to this converter generating speed and torque characteristic parameters. The architecture and analysis was performed using the MATLAB Simulink software, which uses the powergui function to create time-based graphs.

Keywords: MMC (Modular Multilevel Converter), PWM (Pulse Width Modulation), PI (Proportional Integral gain) MATLAB (Matrix Laboratory), powergui (Power graphical user interface), Induction Motor

1. Introduction

There are many different types of multilevel converters with structural differences and also control differences. All these converters are used to convert a fixed DC into a single phase or three AC phases with reduced harmonic distortion. Each converter has its pros and cons when it comes to harmonics, efficiency, economy, reliability, etc. These multilevel converters use capacitors as voltage dividers to create voltage levels at the output voltage. Some of the most common multilevel variables are transformed into an H-bridge converter [1], a diode clamp converter, a flying capacitor converter. For each converter, the number of small modules determines the output power levels, the higher the levels the lesser the harmonics in the voltage and current outputs. In the new era of the 21st-century modular multilevel converters (MMC) [2] are introduced which are replacing most of the above-mentioned multilevel converters with increased reliability and a decrease in cost for manufacturing. Even MMC uses capacitors to separate the electrical energy and to make the energy levels out. Like standard converters, the number of small modules raises the level of the MMC output voltage.

MMC is controlled using two modulation techniques which are sinusoidal PWM and space vector PWM. The sinusoidal PMW technique is the most commonly used PWM technique [3] in most of the converter for conversion of DC to AC (inverting). The space vector PWM technique is considered to be digital PWM with precise pulse generation helps to increase the output voltage magnitude and decrease of harmonics. The MMC can be controlled using two different types of modulation methods which are carrier phase disposition and carrier level-shifted. The optimization of MMC can be easily achieved by utilizing the carrier level shifted space vector PWM technique providing flexibility to the converter reducing harmonics. The proposed MMC with half-bridge sub-modules can be observed below in figure 1.

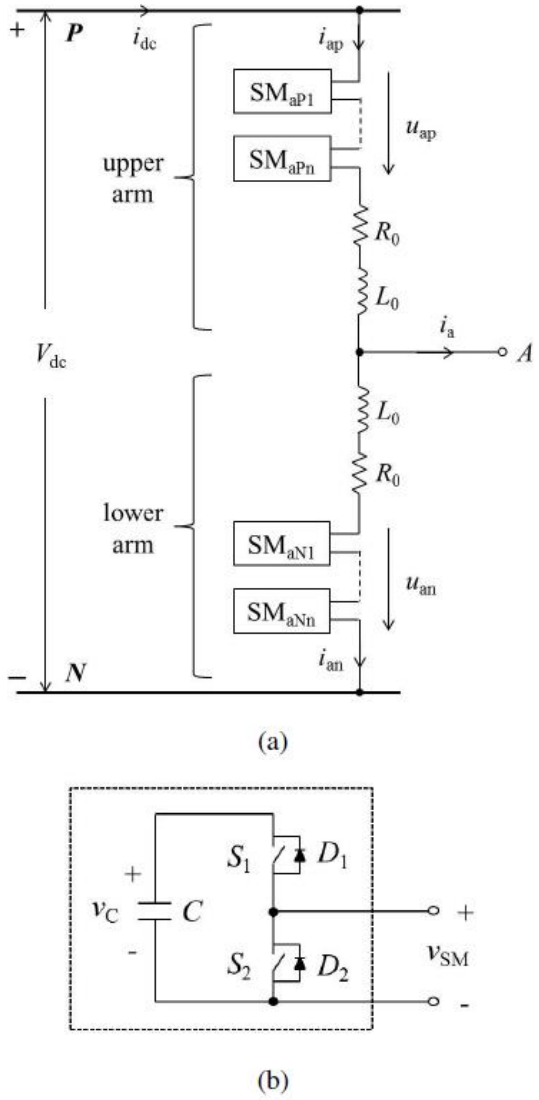

Fig. 1: a) MMC of single-phase b) sub-module internal circuit

The switches S1 and S2 used in the sub-module can be either IGBT or MOSFET for fast switching frequency. The DC side is attached with a capacitor which divides the input voltage in average to the no. of sub-modules [3] connected in a single phase. The upper arm is considered to be a positive set and the lower arm is considered to be a negative set. Elaborating, the upper sub-modules (SMaP1 – SMaPn) generate a positive output voltage, and lower sub-modules (SMaN1 - SMaNn) generated negative output voltage. The output voltage of phase A [4] (V_A) is given as

$$V_A = V_{Ao} - L_o/2 \, . \, di_A/dt - R_o/2 \, . \, i_A \quad \text{.....(1)}$$

$$V_{Ao} = (V_{dc} - U_{ap} + U_{an})/2 \quad \text{.....(2)}$$

Here, Vdc is the input DC voltage magnitude, Lo and Ro are the inductance and resistance of the leg branch, i_A is the phase current, U_{ap} and U_{an} are the upper and lower cumulative total voltage [5] of sub-modules.

The input to the MMC converter can be any DC source like a battery or renewable sources like PVA, wind farm, fuel cell. In most applications, renewable energy sources are used for the utilization of renewable power [6] in AC loads. In our proposed circuit topology PVA source is considered as an input source for running a three-phase induction machine [8]. In this paper, the modeling of capacitor balance control structure (with PI and fuzzy) is discussed in section II followed by carrier level shifted space vector PWM technique integration to the capacitor balance controller explanation in section III. Section IV includes the simulation results and analysis of the proposed circuit topology with different controllers comparison, concluding with section V along with references.

2.Capacitor Balance Control

The capacitor balance control is used to generate a reference signal for the carrier level shifted space vector PWM to control the MMC switches for balanced capacitor voltages in each sub-module. The reference signal generated from the controller tends to maintain the voltages of capacitors [7] in the sub-modules are a specific user-defined reference voltage level. The MMC considered for the modeling and testing is a three-phase four sub-modules in each phase MMC circuit. Which defines the upper arm [7] of one of the phases include two sub-modules and the lower arm also include two sub-modules. The total number of sub-modules utilized is 12 for three-phase MMC. The proposed capacitor balance controller for the MMC is shown below in figure 2.

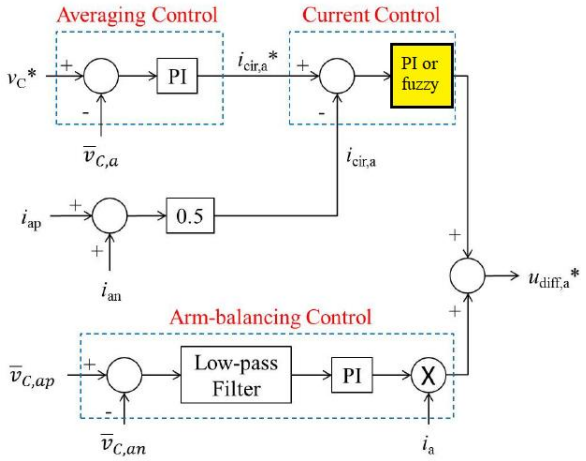

Fig. 2: Capacitor voltage balance controller

As observed in the above control structure the current controller is updated with sensible intuitive controls for better control of the controller. The control structure takes input from one of the measured capacitor voltage (Vca) which is compared to user-defined reference capacitor voltage value Vc* [8]. An error is given to the PI control to create a reference to rotating the current i_{cira}. Current reference compared to the current time of the current upper arm i_{ap} and the lower arm i_{an} provided as

$$i_{cira} = (i_{ap} + i_{an})/2 \quad \text{.....(3)}$$

The error generated by this comparison is fed to the PI controller or fuzzy logic control generating a reference signal for circulating current. For the arm balance control, upper arm cumulative capacitor voltages are compared to lower arm cumulative capacitor voltage, with error generation fed to PI controller through low pass filter for reduction of disturbances in the signal. The reference current magnitude is multiplied by the phase current i_a for the generation of arm balancing reference signal. Both the signals are added up for the final reference signal given as input to carrier level shifted space vector PWM [9].

Fuzzy logic controller:

The fuzzy interface system is considered to be an advanced controller as compared to the PI controller as it generates near value for the given input with a faster response rate. A quick and strong response of the controller improves the performance of the controller and the settling of the system is reduced. For our system when the current controller is replaced with a fuzzy system the reference generation will become faster and the capacitor voltages settle faster as compared to the PI controller. The fuzzy interface system adopted into the proposed control structure has one input variable and one output variable. 'Mamdani's fuzzy interface design is considered for this purpose by including inputs that include seven gauss membership functions and seven triangular output

membership functions. The entry and removal functions are shown in Figure 3 below.

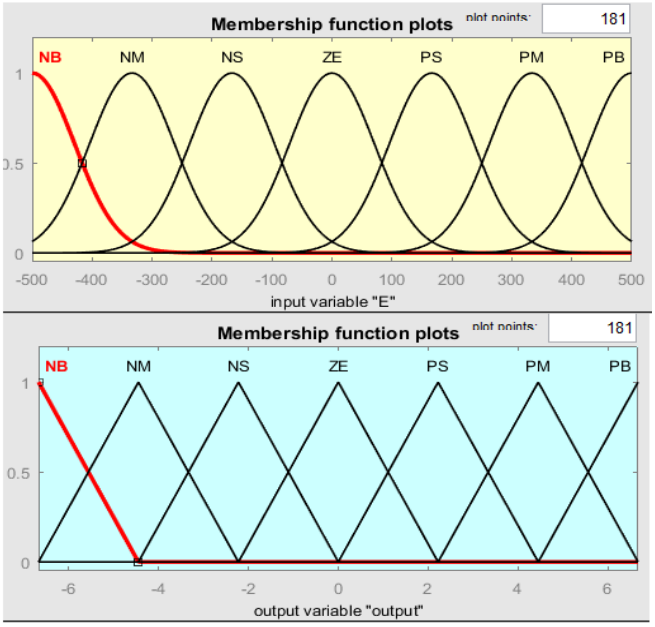

Fig. 3: Input and output functions of sensitive visual system membership

The input variable is set in the range between -500 to 500 which is defined as per the input error. The output variable is set between the range -6.66 to 6.66 which is defined as per the PI controller Kp and Ki gains. The seven membership functions in both variables are named as per the position in the range given. NB – Negative Big, NM – Negative Medium, NS – Negative Small, ZE – Zero, PS – Positive Small, PM – Positive Medium, PB – Positive Big. The 7 rules set for these membership functions are linear given as, If 'E' is NB 'output' is NB, If 'E' is NM 'output' is NM, If 'E' is NS 'output' is NS, If 'E' is ZE 'output' is ZE, If 'E' is PS 'output' is PS, If 'E' is PM 'output' is PM, If 'E' is PB 'output' is PB. The rule base for the above fuzzy controller is shown below.

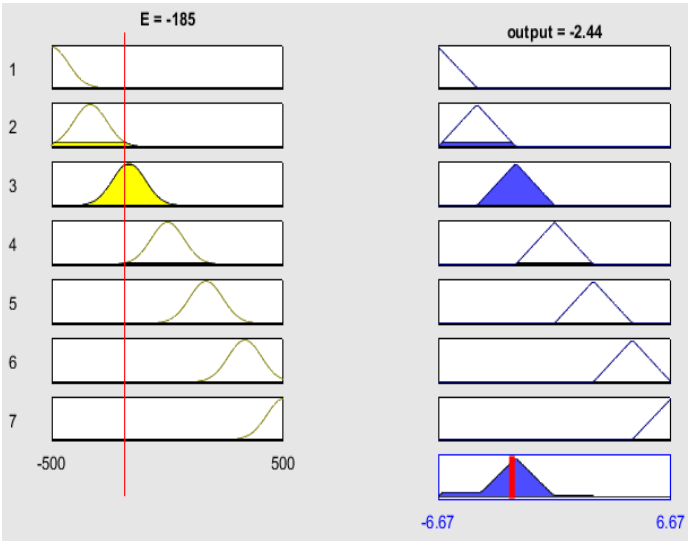

Fig. 4: Proposed linear fuzzy rule base

3.Space Vector Pwm Optimization

The space vector PWM [11] technique is an advancement to the traditional sinusoidal PWM technique as it uses digitalized switching pulse generation concerning the sector selection. The switching sequence for the switches will be given by digital sets [12] as per the requirement of the output voltage waveform. A General space vector sector generation can be seen below.

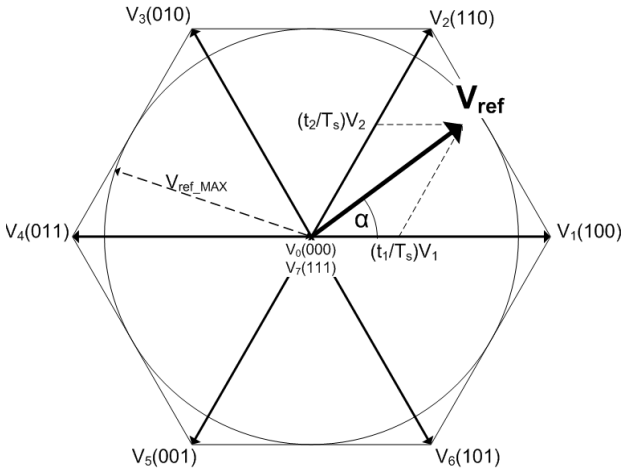

Fig. 5: General space vector section generation

The above sector selection [13] concerning reference voltage from the capacitor voltage balance controller Vref generates the pulses for the upper arm and lower arm bridges. Reference base signal for space vector PWM is given as

$$V_{sv} = V_{sin} - (V_{max} + V_{\min})/2 \text{ ……..(4)}$$

Vsin is the user-defined sinusoidal reference with the fundamental frequency given as per the requirement. The pulses generated for the MMC are given as shown below.

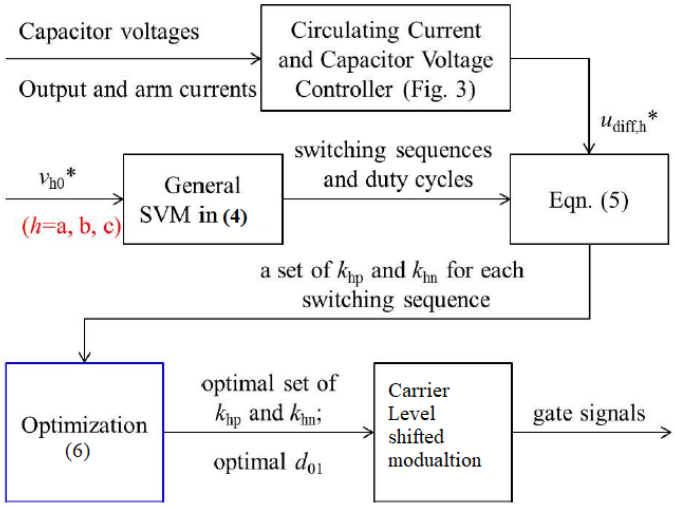

Fig. 6: MMC controller with space vector optimization

The below equation determines the selection of reference values as per the difference voltage reference generated from the capacitor voltage balance controller.

$$k_{hi} = \begin{Bmatrix} round\ (k_{hi}^*), & if\ (0 < k_{hi}^* < n); \\ 0, & if\ (k_{hi}^* \le 0); \\ n, & if\ (k_{hi}^* \ge n). \end{Bmatrix} \text{…...(5)}$$

Here k_{hi}^* represents the reference value selection and 'i' represents a,b, or c phases. The variable 'n' represents many sub-modules. The final reference signal is optimized between certain limits to generate pulses for the converter when compared to carrier level shifted modulation signals. The optimization of the reference signal is given as

$$d_{o1} = \begin{Bmatrix} d_{opt}, & if\ (0 \le d_{opt} \le d_o \\ 0, & if\ (d_{opt} < 0); \\ d_o, & if\ (d_{opt} > d_o). \end{Bmatrix} \text{ …….. (6)}$$

The final reference signal and the comparison of the carrier level shifted triangular waveform is represented as in figure 7.

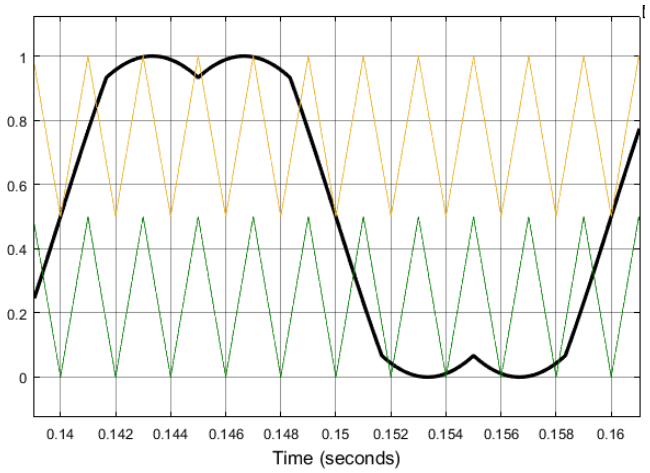

Fig. 7: Space vector reference signal comparison to carrier level shifted PWM

With the above control modules and proposed MMC the complete circuit is modeled and controlled with PVA input and induction motor load in the next section align with graphical representations.

4.Simulation Results

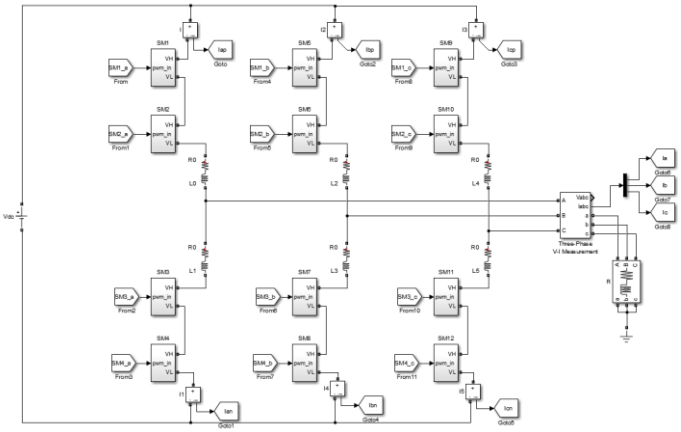

Fig. 8: Modeling of proposed MMC

The above figure 8 is the modeling of the proposed four sub-modules MMC connected to a static load. The pulses for the MMC are made by the capacitor balance controller as shown below.

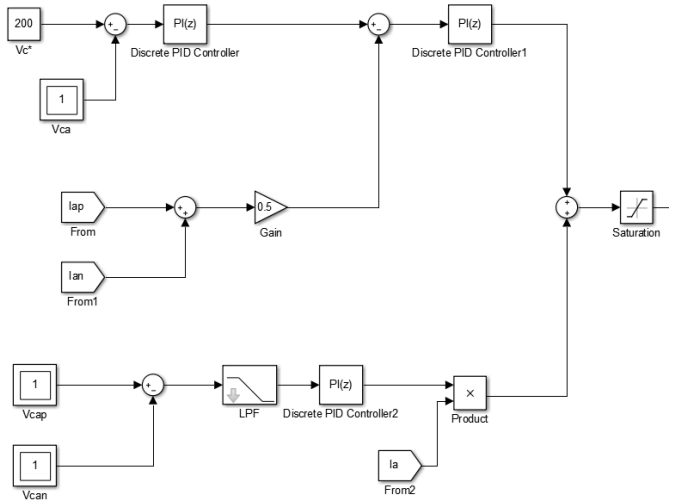

Fig. 9: Capacitor voltage balance control modeling

Simulation with the above modules is run for 4secs and the capacitor voltages of three phases are recorded. The reference voltage in the controller is set at 200V which makes the voltages of the capacitors stabilize at 200V.

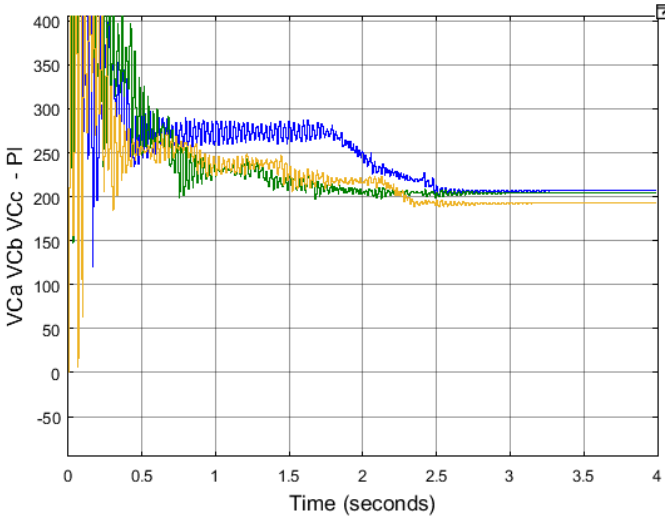

Fig. 10: Capacitor voltages of phase a, b, and c with PI controller

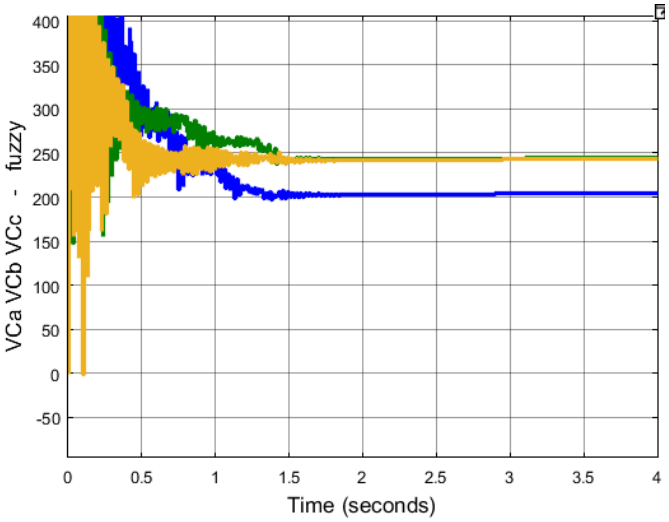

Fig. 11: Capacitor voltages of phase a, b, and c with fuzzy controller

As seen the Figures 10 and 11 the power capacitor of a, b, and c phases (VCa VCb VCc) with PI and fuzzy logic controller, the voltage settles faster and maintains stability for the fuzzy controller. The settling time for the PI controller is 2.5sec whereas the settling time for fuzzy is noted at 1.5secs.

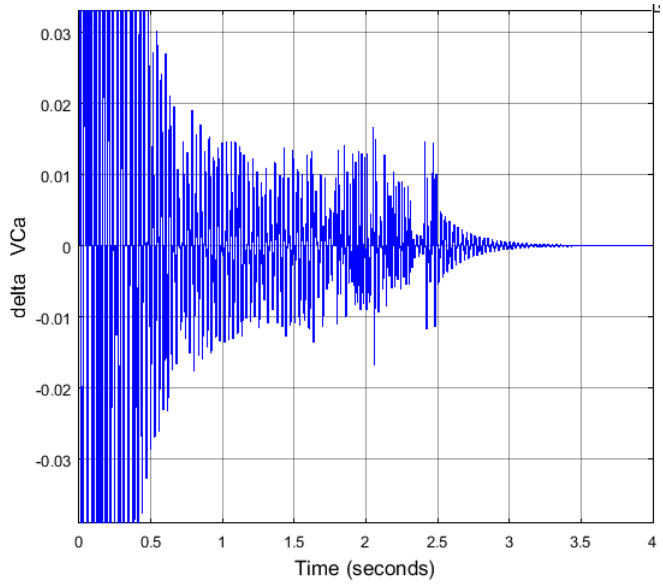

Fig. 12: Switch to C_a capacitor power with PI control

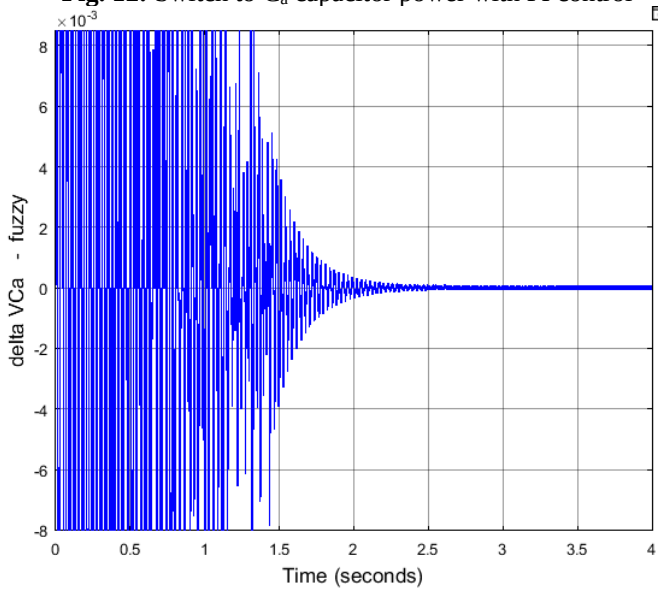

Fig. 13: Switch to the capacitor of C_a with a fuzzy controller

Similar to the capacitor voltages the change in capacitor voltages ΔVCa of fuzzy controller settles faster as compared to PI controller. The circuit is updated with a PVA source at the input and induction motor on the load side. The characteristics of the circuit modules are recorded and plotted to time.

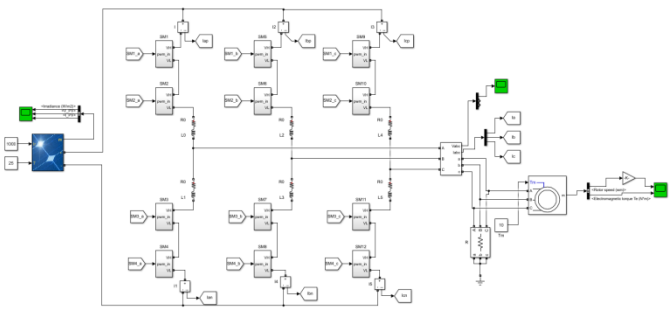

Fig. 14: Proposed MMC with PVA input and induction motor load

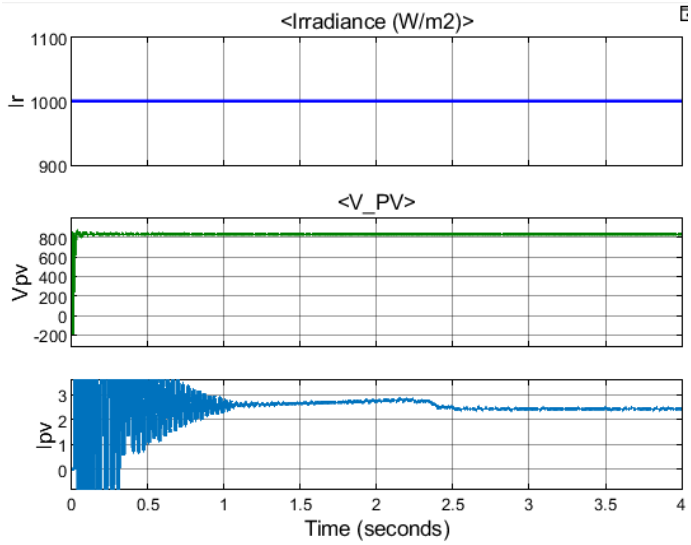

Fig. 15: PVA characteristics

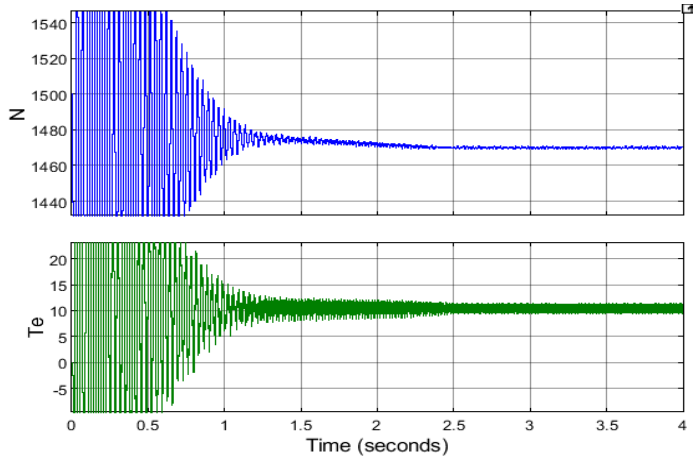

Fig. 16: Induction motor characteristics

The parameters of PVA and IM are given in the Appendix section.

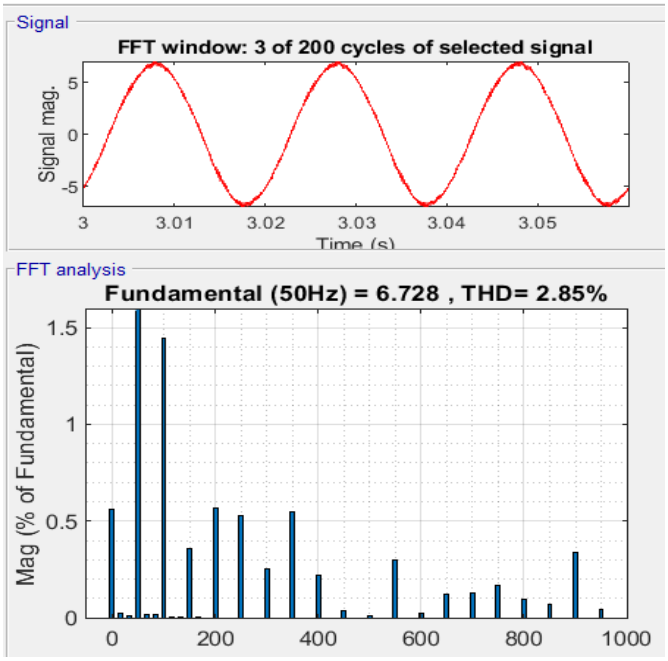

Fig. 17: THD of stator current of IM using an FFT analysis tool

5.Conclusion

With the above results and discussion, it is clear that the capacitor voltages are balanced at 200V as per the reference given by the user. The voltages of the capacitor even settle faster for a fuzzy controller as compared to a PI controller. The settling speed is 1sec faster as compared to the conventional controller. The THD of stator current when the MMC is connected with PVA and induction motor is noted which is less than 5%. The PVA and induction motor characteristics are studied when the machine is operated with nine levels of three-phase AC voltage.

6.Appendix

PVA parameters :

Vmp = 54.7; Voc = 64.2V; Imp = 5.58A; Isc=5.96A; Pmp = 305W; Ns = 13; Np = 50.

IM parameters :

Pnom = 4kW; Vnom = 400V; fnom = 50Hz; Rs = 1.405ohms; Rr= 1.395ohms; Lls = Llr = 0.005839H; Lm = 0.1722; J = 0.0131; p = 2.

References

1. Ilves, K et.al.,: ‘Comparison of cascaded multilevel converter topologies for AC/AC conversion’. 2014 Int. Power Electronics Conf. (IPEC-Hiroshima 2014 – ECCE-ASIA), Hiroshima, Japan, May. 2014, pp. 1087–1094
2. Hagiwara et.a.,l: ‘A medium-voltage motor drive with a modular multilevel PWM inverter’, IEEE Trans. Power Electron., 2010, 25, (7), pp. 1786–1799
3. Korn, A.et.al. ‘Low output frequency operation of the modular multi-level converter’. 2010 IEEE Energy Conversion Congress and Exposition (ECCE), Atlanta, USA, 12–16 September 2010
4. Espinoza, M., Espina, E., Diaz, M., et al.,: 'Improved control strategy of the modular multilevel converter for high power drive applications in low-frequency operation'. 2016 18th European Conf. on Power Electronics and Application (EPE), Karlsruhe, Germany, Sep. 2016, pp. 5–9
5. Li, B., Zhou, S.,et al.,: 'An improved circulating current injection method for modular multilevel converters in variable-speed drives, IEEE Trans. Ind. Electron., 2016, 63, (11), pp. 7215–7225
6. Karanayil, B., et.al.,: 'Performance evaluation of three-phase grid-connected photovoltaic inverters using electrolytic or polypropylene film capacitors, IEEE Trans. Sustain. Energy, 2014, 5, (4), pp. 1297–1306, DOI: 10.1109/TSTE.2014.2347967
7. Espinoza, M., Espina, E., Diaz, M., et al.,: ‘Control strategies for modular multilevel converters driving cage machines’. 2017 IEEE 3rd Southern Power cage machines’. Electronics Conf. (SPEC), Puerto Varas, Chile, Dec 2017, pp. 1–6
8. Sau, S.et.al.,: ‘Modular multilevel converter based variable speed drives with constant capacitor ripple voltage for wide speed range’. IECON 2017 – 43rd Annual Conf. of the IEEE Industrial Electronics Society, Beijing, China, Oct. 2017, pp. 2073–2078, DOI: 10.1109/IECON.2017.8216348
9. Q. Tu, Z. Xu, et.al., "Reduced Switching-Frequency Modulation and Circulating Current Suppression for Modular Multilevel Converters," IEEE Trans. Power Del., vol. 26, no. 3, pp. 2009–2017, Jul. 2011.
10. J. Mei, B. Xiao, et al., “Modular Multilevel Inverter with New Modulation Method and Its Application to Photovoltaic Grid-Connected Generator,” IEEE Trans. Power Electron., vol. 28, no. 11, pp. 5063-5073, Nov. 2013.
11. Y. Deng, et.al., “A Fast and Generalized Space Vector Modulation Scheme for Multilevel Inverters,” IEEE Trans. Power Electron., vol. 29, no. 10, pp. 5204-5217, Oct. 2014.
12. K. H. Teo, et.al., “A Fast and Generalized Space Vector PWM Scheme and Its Application in Optimal Performance Investigation for Multilevel Inverters,” in Proc. IEEE Energy Conversion Congress and Exposition (ECCE), Sept. 2013, pp. 3977-3983.
13. R. G. Harley, et.al., "Space Vector Modulation Method for Modular Multilevel Converters," in Proc. Annual Conference of IEEE Industrial Electronics Society (IECON), Oct./Nov. 2014, pp. 4715-4721.